

Xiao Caide · Sen-Fang Sui

Numerical simulations of surface plasmon resonance system for monitoring DNA hybridization and detecting protein-lipid film interactions

Received: 4 May 1998 / Revised version: 27 July 1998 / Accepted: 27 August 1998

Abstract This paper presents a simple method to extract information about thin organic films from surface plasmon resonance (SPR) spectra. From numerical simulations it was found that a shift ($\Delta\theta_{\text{SPR}}$) of an absorption peak in the SPR spectrum was directly proportional to the product of the thin organic film thickness and the refractive index difference between the thin organic film and a buffer soaking the sample. It was also found that $\Delta\theta_{\text{SPR}}$ was not sensitive to the thin organic film support of a gold film and a glass cover slip. Relationships between $\Delta\theta_{\text{SPR}}$ and distributions of macromolecule structures, in the thin organic films were theoretically established. Formulae were derived for a homemade SPR system to calculate length, transverse area, density and surface concentration of macromolecules in the thin organic film. The validity of these treatments was checked by precisely measuring the size of a single distearoylphosphatidylcholine molecule on a gold-supported phospholipid film; by quantitatively monitoring hybridization of synthesized oligonucleotides strands based on a biotin/avidin system; and by quantitatively detecting the steric hindrance of rabbit C-reactive protein specifically bound to phospholipid monolayers composed of synthesized lipids.

Key words Surface plasmon resonance · Numerical simulation · Supported film

Abbreviations *bDNA1*, *DNA1c*, *bDNA2*, *DNA2c* Four synthesized oligonucleotide single strands · *DPPC* Dipalmitoylphosphatidylcholine · *DPPE* Dipalmitoylphosphatidylethanolamine · *DPPEB* A synthesized phospholipid acting as a receptor for avidin ($\text{DPPE} + \text{NHSB} \rightarrow \text{DPPEB}$) · *DSPC* Distearoylphosphatidylcholine · *DS8PC*, *DS6PC*, *DP3PC* Three synthesized phospholipids acting as receptors for rCRP · *NHSB* N-Hydroxysuccinimidobiotin · *PC* Phosphorylcholine · *PE-sepharose 4B* Sepharose with phosphatidylethanolamine residues for rCRP purification · *rCRP* Rabbit C-reactive protein · *SPR* Surface plasmon resonance

tidylethanolamine · *DPPEB* A synthesized phospholipid acting as a receptor for avidin ($\text{DPPE} + \text{NHSB} \rightarrow \text{DPPEB}$) · *DSPC* Distearoylphosphatidylcholine · *DS8PC*, *DS6PC*, *DP3PC* Three synthesized phospholipids acting as receptors for rCRP · *NHSB* N-Hydroxysuccinimidobiotin · *PC* Phosphorylcholine · *PE-sepharose 4B* Sepharose with phosphatidylethanolamine residues for rCRP purification · *rCRP* Rabbit C-reactive protein · *SPR* Surface plasmon resonance

Introduction

The surface plasmon resonance (SPR) technique has been widely used in recent years to quantitatively monitor ligand-receptor interactions in real time (Liedberg et al. 1995). Surface plasmons are electric charge density waves that propagate along an interface between a metal and a dielectric. A commonly used method to excite surface plasmons was initially suggested by Kretschmann (Raether 1989). In the Kretschmann configuration a prism is used as a coupler between incident photons and surface plasmons in a thin metal film (see Fig. 2 below). In the condition $\theta > \theta_c$, total light reflection would occur in the system. If the incident light was in a p-polarized mode, then incident photons might excite surface plasmons at an incident angle. This angle was called the resonance angle (θ_{SPR}). Because there was energy transfer from incident photons to surface plasmons in the resonance condition, the light reflectivity (*R*) would decrease to almost zero at the resonance angle. This optical phenomenon was called surface plasmon resonance. A *R* versus θ graph with a deep absorption peak caused by SPR was called a SPR spectrum.

Because there are multilayered optical media in a SPR system, relationships between SPR spectra and optical parameters are very complex. There is not a simple method to solve SPR spectra. Empirical formulae (Stenberg et al. 1991) are usually used to extract sample information from SPR spectra. One empirical formula from one SPR system may not be suitable for another SPR system. Even in the

X. Caide · S.-F. Sui
The State Key Laboratory of Biomembrane
and Membrane Biotechnology,
Department of Biological Science & Biotechnology,
Tsinghua University,
Beijing 100084, China

X. Caide (✉)
Yunyang Medical College, Shiyan 442000, Hubei, P.R. China
e-mail: xiaocd@iname.com

of the gold film was measured at first in air, then the cover slip was taken away from the prism. After the water on the glass side of the cover slip had evaporated, there was a lipid monolayer transfer process as described above. The cover slip was stuck on the base of the prism by water, and the SPR spectrum was measured in air again. From the shifts of the SPR spectra, it was easy to judge the existence of a lipid monolayer on the gold film.

Generally, monolayers of neutral phospholipids with longer chains could be easily transferred to the gold film. In fact it was easy to know if there was a lipid monolayer on the gold film just by visual inspection. After the horizontal transfer process, if a thin water layer could be seen on the gold film, then there was no problem for the lipid monolayer transfer. Usually a water drop could not spread over the gold film.

The cover slip with the gold film and lipid monolayer was removed from the prism, and held in the air. After water on the cover evaporated, the cover slip was stuck to the prism base by a drop of index matching oil. A chamber was installed in the SPR system, and the chamber was filled with buffer. The quality of the monolayer on the gold film could also be checked by ellipsometry.

The optical layout of a homemade SPR system

The optical layout of the homemade SPR system is shown in Fig. 2. A cover slip, a gold film and a sample layer constituted a sensitive chip. The chip was stuck to the base of the prism by an index matching oil. An "O" ring and a Teflon chunk were pressed against the sensitive chip, forming a 200 μl chamber. There were two channels in the Teflon chunk for pumping a required sample liquid into the chamber.

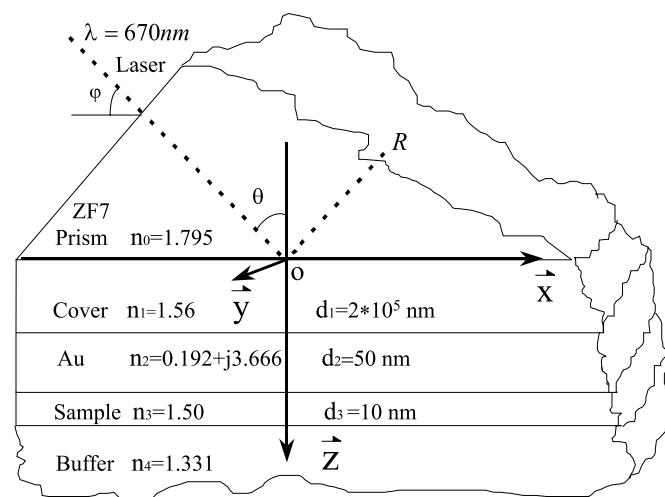


Fig. 2 An optical layout of a homemade SPR system. Parameters of each optical medium are marked. The dashed line represents a p-polarized light beam emitted from a laser diode fixed on one side of a goniometer. Vectors x , y and z represent axes of a coordinate in the optical system. A PC/XT computer was used to control the goniometer and record the SPR spectra

In the SPR system shown in Fig. 2 there are five optical media: the prism, the glass cover slip, the gold film, the sample and the buffer. Their optical refractive indexes are represented by elements of the matrix $n = [n_0, n_1, \dots, n_4]^T$. The quantitative value of each element is marked inside the figure. The prism was made from a piece of ZF7 glass. Its refractive index at a given λ was calculated according to the formula $n = 1.758 + 16640/\lambda^2$. The refractive index of the microscope glass cover was 1.56. The refractive index of the gold film at a given λ was obtained from the following formula:

$$n = \sqrt{(30.3723 - 0.065272 \lambda) + j(17.1691 - 0.0468757 \lambda + 3.48485 \times 10^{-5} \lambda^2)}.$$

This formula was derived from data in Raether (1989). The buffer refractive index was chosen as 1.331 for water at room temperature. Optical media thicknesses were represented by elements of the matrix $d = [d_0, d_1, d_2, d_3, d_4]^T$. Only d_1, d_2 and d_3 were used in the numerical simulations.

The optical system was built on an X-ray diffraction goniometer. A coordinate of the optical system was constructed by the vectors x , y and z in Fig. 2. A laser diode (Hitachi, HL671G) was fixed on one side of the goniometer. A laser beam was reflected from the base of the prism to a silicon photocell which was installed on a large rotatable plate of the goniometer. The prism was installed on a small rotatable plate of the goniometer. The two plates were coaxial. The variable ϕ represented an angle between the x axis and the laser beam from the diode. The small plate rotated around axis y at a speed of $d\phi/dt = 0.500^\circ/\text{s}$, and the larger plate rotated at double speed to track the reflected light. Reflected light intensity signals were amplified to 0–5 V, converted to digital form and recorded in a PC/XT computer. In the homemade SPR system, ϕ was a directly measured parameter. Values of the incident angle θ were derived from the formula

$$\theta = 45^\circ + \arcsin\left(\frac{1}{n_0} \sin(45^\circ - \phi)\right).$$

In the condition $35^\circ < \phi < 60^\circ$ the two angle parameters had a perfect linear relationship, $d\theta/d\phi = -0.550$. The measurement accuracy of parameter ϕ in the homemade SPR system was 0.001° .

Theory

A numerical simulation program written in MathCAD plus6 is available from the author. In the program, $R(\theta, \lambda, n, d)$ is a reflectivity function of the SPR system. This function was defined according to Fresnel's formulae. From this function, SPR spectra for a given set of λ, n, d could be obtained. Another function $\theta_{\text{SPR}}(\lambda, n, d)$ in the program was defined to find a root of the equation $dR(\lambda, \theta, d, n)/d\theta = 0$; a root of the equation was θ_{SPR} . Because the derivative $dR(\lambda, \theta, d, n)/d\theta$ would change sign around θ_{SPR} , the program was designed to check the sign and magnitude of the derivative from an initial angle θ_0 ($\theta_0 > \theta_c$)

in a step $\Delta\theta$ until $|dR(\lambda, \theta, d, n)/d\theta| < \varepsilon$. The parameter ε was a calculation error tolerance for determining θ_{SPR} . In the beginning the program searched θ_{SPR} in a forward direction if $dR(\lambda, \theta, d, n)/d\theta < 0$, and vice versa. From an angle where the derivative changed sign, the program would search θ_{SPR} in a reverse direction with a smaller step.

From the simulations it was found that for $d^2R(\lambda, \theta, d, n)/d\theta^2 > 30$ around θ_{SPR} (units in degrees) in the homemade SPR system, a calculation error for determining θ_{SPR} would be smaller than 0.001° in the condition $\varepsilon = 0.03$. This root searching process was only suitable for SPR spectra in the condition $d_1 = 0$. In this condition, SPR spectra were smooth, and the equation $dR(\lambda, \theta, d, n)/d\theta = 0$ had a single root by the incident angle around a SPR absorption peak.

A glass cover slip was used as a support for the gold film. Because the refractive index of the cover slip was lower than the refractive index of the prism, light beams reflected from the prism/cover slip interface and the cover slip/gold interface had a phase difference:

$$\delta = 4\pi \frac{d_1}{\lambda} \sqrt{n_1^2 - n_0^2 \sin^2 \theta}.$$

As the incident angle θ would change in an angle scan process for SPR spectra, δ would fluctuate between 0 and 2π . A noise-light interference signal would combine with the SPR spectra. The noise frequency was

$$f = \frac{\pi}{180} \frac{d_1}{\lambda} \frac{n_0^2 \sin 2\theta}{\sqrt{n_1^2 - n_0^2 \sin^2 \theta}} \frac{d\theta}{dt}.$$

From a Fourier transform it was found that the noise frequency was as large as 30 times the frequency of a SPR spectrum. In the homemade SPR system the noise frequency was about 7 Hz. Because the interference noise could be filtered out by software and/or hardware, the effect of the cover slip was ignored in the numerical simulations for θ_{SPR} . Higher refractive index prisms should be used to suppress the noise.

From the parameters marked in Fig. 2 (except $d_1 = 0$), a family of θ_{SPR} versus d_3 curves was obtained by numerical simulations, and these are shown in Fig. 3. The sample refractive index values are marked on the figure. These curves were very similar to current-voltage curves of a bipolar transistor. In each of the curves one could distinguish three regions: a saturated region ($d_3 > 400$ nm), a non-linear region ($10 \text{ nm} \leq d_3 \leq 400$ nm) and a linear region ($d_3 \leq 10$ nm). In most cases the SPR system for biological applications worked in the linear region. In the linear region, as shown in the inset of Fig. 3, a shift of a SPR spectrum peak ($\Delta\theta_{\text{SPR}}$) was directly proportional to the product of the sample film thickness and the refractive index difference between the sample and the buffer soaking the sample:

$$\Delta\theta_{\text{SPR}} = 0.571 \times (n_3 - n_4) \times d_3 \quad (1)$$

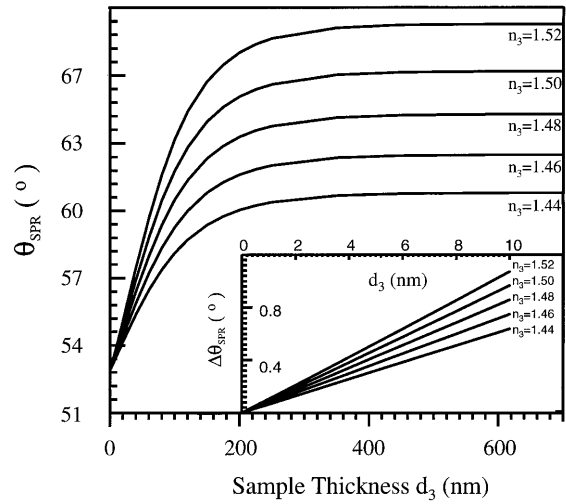


Fig. 3 Numerical simulation results about resonance angle θ_{SPR} and sample thickness d_3 for five given sample optical refractive indexes. Other optical parameters for numerical simulations are shown in Fig. 2, except the glass cover thickness d_1 was set to zero. The *inset* in the figure is a zoom of a linear region of the curves. In this region, $\Delta\theta_{\text{SPR}}$ was directly proportional to the product of the sample film thickness and the refractive index difference between the sample and a buffer containing the sample

From numerical simulations it was found that the application of Eq. (1) could be extended to the conditions: $40 \text{ nm} \leq d_2 \leq 90 \text{ nm}$, $d_3 \leq 10 \text{ nm}$, $1.330 \leq n_3 \leq 1.52$ and $n_4 = 1.331 \pm 0.001$. In these conditions an average and a standard deviation of the ratio $\Delta\theta_{\text{SPR}} / ((n_3 - n_4) \times d_3)$ were 0.571 and 9.64×10^{-3} , respectively. The condition $40 \text{ nm} \leq d_2 \leq 90 \text{ nm}$ meant that gold films with thickness between 40 nm and 90 nm gave the same results for $\Delta\theta_{\text{SPR}}$. Although there was no limit to the gold film thickness, a gold film of 50 nm thickness was the best for producing a SPR spectrum with the deepest absorption peak. A deep and sharp absorption peak gave higher accuracy for determining the value θ_{SPR} . Equation (1) may be widely used for monitoring biological samples in water environments, because refractive indexes of biological samples are usually below 1.52, their thickness is less than 10 nm, while the refractive indexes of most buffer solutions is 1.331 at room temperature.

In the SPR system, biological samples a usually concentrated in a layer with a thickness less than 10 nm, and sample molecules might no compact to form a homologous film. The sample surface concentration (σ) was a better parameter than sample index n_3 and sample thickness d_3 . A variable C was used as the sample volume concentration in the sample layer. By multiplying C to both sides of Eq. (1), a formula for σ and $\Delta\theta_{\text{SPR}}$ was derived (noticing that $\sigma = C \times d_3$):

$$\sigma = \frac{1}{0.571} \frac{C}{n_3 - n_4} \Delta\theta_{\text{SPR}}. \quad (2)$$

For protein samples the ratio of $C/(n_3 - n_4)$ was between 5 and 7. If the ratio was chosen as 5.71, then a simple formula was obtained. This formula was first represented by

Stenberg et al. (1991) by using radiolabelled proteins:

$$\sigma = 10 \Delta\theta_{\text{SPR}}. \quad (3)$$

If a molar mass (M) of a sample molecule was given in a unit of g/mol, then a formula for a sample molecule number (N) per square millimeter in the sample film was derived, and formula for a sample molecule transverse section area (S) in a unit of \AA^2 was obtained:

$$N = 6.023 \times 10^{15} \frac{\Delta\theta_{\text{SPR}}}{M}, \quad (4)$$

$$S = \frac{1}{60.23} \frac{M}{\Delta\theta_{\text{SPR}}}. \quad (5)$$

Results and discussion

Measuring supported phospholipid films

Phospholipid films transferred from a Langmuir-Blodgett trough onto a solid surface are called supported films. Gold-supported phospholipid films were studied at first, because they were the basis of macromolecule assembly experiments. As the components of a phospholipid monolayer on an air/water interface of a Langmuir-Blodgett trough could be precisely controlled, the supported film could be used as a model to study lipid-protein interactions and macromolecular assemblies. A SPR spectrum of a base gold film in the buffer is shown in the inset of Fig. 4 by the curve marked with "1". When curve 1 was measured, the SPR system was set in a mode to automatically measure the shift of the resonance angles. After 1100 s the mea-

surement was paused. A DSPC monolayer was horizontally transferred onto the same gold film, and the measurements were continued. The DSPC monolayer on the gold film caused changes in the SPR spectrum: the resonance angle shift was 0.270° (Fig. 4). After 2400 s, another SPR spectrum was measured (curve 2 in the inset of Fig. 4).

The molar mass of the DSPC was 790 g/mol. By ellipsometry it was found that the refractive index of the DSPC film was 1.45. From Eq. (1) and Eq. (5), the thickness of the DSPC film was found to be 3.98 nm and the area occupied by a DSPC polar group at the lipid/water interface was found to be 48 \AA^2 . From a book (Chapman and Wallach 1973) it was found that a polar head of DPPC occupied 48 \AA^2 in a lipid/water interface by X-ray diffraction, and the thickness of a DPPC film in water was 3.65 nm from Langmuir-Blodgett technique. As the length of one pair of CH_2 was 0.25 nm (Chapman 1968), the thickness of one DSPC film should be 4.15 nm. The above SPR measurements agreed well with these experimental results.

Monitoring oligonucleotide hybridizations in real time

Analysis of DNA and DNA-protein complexes are essential in clinical diagnostics, and in the pharmaceutical industry (Sheila 1993). Traditional methods to immobilize DNA on solid surfaces are often based on adsorption or covalent bonds, which are difficult to control. In the present work biotin-labelled single strands of oligonucleotides were immobilized on a biotin/avidin system, and hybridization of oligonucleotide strands was observed in real time by the homemade SPR system.

In previous work (Liu 1995) it had been demonstrated that the specific binding of avidin molecules to supported monolayers containing DPPEB was obviously dependent on the molar ratio of DPPEB to DPPE. The ratio 1:12 was found to be optimal for the monolayer with the mixed lipids to specifically bind avidin molecules. For this reason, supported films composed of DPPEB and DPPE in a molar ratio of 1:12 were prepared for the sensitive chips. Avidin liquid (10 μl , 1.0 mg/ml) was injected into the chamber containing 150 μl buffer. In 60 min the adsorption of avidin on the chip became saturated. Then the chamber was washed to remove free avidin molecules, and 140 μl of buffer were injected inside the chamber again. It was found that $\Delta\theta_{\text{SPR}} = 0.253^\circ$.

Biotin-labelled oligonucleotide bDNA2 liquid (10 μl , 2.0 mg/ml) was added to the chamber; 120 min later the chamber was washed with buffer, then 130 μl buffer was added inside that chamber. It was found that $\Delta\theta_{\text{SPR}} = 0.050^\circ$. DNA2c liquid (10 μl , 2.0 mg/ml) was injected into the chamber. After the adsorption was saturated, the chamber was washed and filled with buffer again. Now the shift of resonance was $\Delta\theta_{\text{SPR}} = 0.044^\circ$. The specific hybridization between bDNA2 and DNA2c was confirmed by cross hybridization of bDNA2 with bDNA1 and DNA1c. No significant change of θ_{SPR} was observed when bDNA1 or

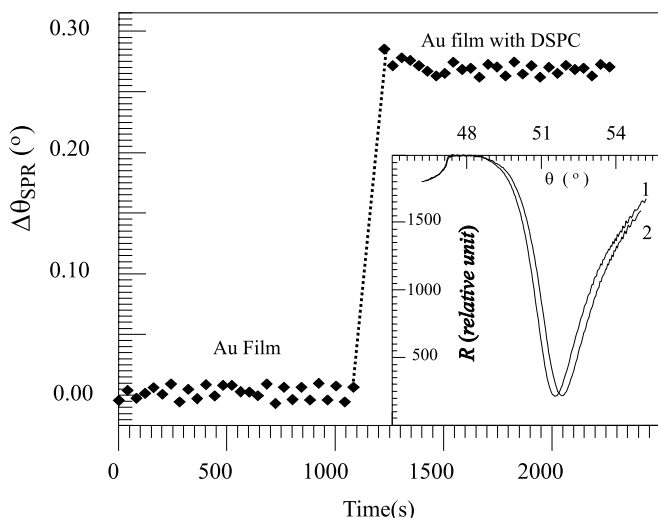


Fig. 4 Relationships between $\Delta\theta_{\text{SPR}}$ and time before and after a DSPC monolayer was transferred onto a gold film. The shift of the SPR spectrum resonance angle caused by a DSPC monolayer was 0.270° . The inset shows a SPR spectrum about a bare gold film (curve 1) and a SPR spectrum about the same gold film with a DSPC monolayer (curve 2)

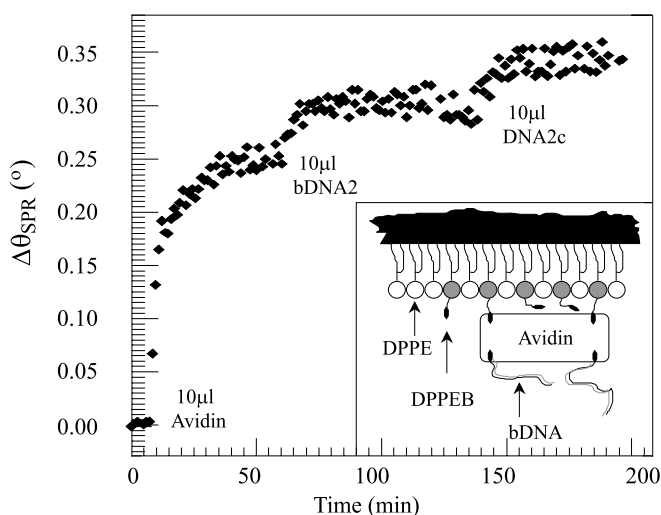


Fig. 5 Relationships between $\Delta\theta_{\text{SPR}}$ and time in the course of the following processes: avidin binding to a DPPEB/DPPE monolayer transferred onto a gold film; bDNA2 binding to avidin film; DNA2c hybridizing with bDNA2. In the end the total resonance angle shift was $0.253^\circ + 0.050^\circ + 0.043^\circ$ (experimental details in the text). The inset is a drawing of the macromolecular assembly on the gold film

DNA1c was added inside the chamber to react with bDNA2 immobilized on the avidin film.

From the values of $\Delta\theta_{\text{SPR}}$ and the molar masses of the samples, experimental results were obtained (Fig. 5). There were $2.464 \times 10^{10}/\text{mm}^2$ avidin molecules binding to the DPPEB/DPPE film, there were $4.898 \times 10^{10}/\text{mm}^2$ bDNA2 strips binding to avidin film and there were $4.176 \times 10^{10}/\text{mm}^2$ DNA2c strips hybridized with bDNA2. The ratios of these numbers were 1.0/1.988/1.695. Because on each side of an avidin molecule there were two biotin binding sites, the ratios meant that almost each avidin molecule bound with two bDNA2 strands, and nearly every bDNA2 strand hybridized with a DNA2c strand. From a two-dimensional crystal structure of avidin (Qin 1995), every square millimeter of an avidin two-dimensional crystal film should contain 2.6×10^{10} avidin molecules. From these data it was easy to conclude that avidin molecules are rather orderly assembled on the chip in the above experiments.

Detecting rCRP and phospholipid film interactions

C-reactive protein (CRP) is a major acute phase reactant in most mammalian species (Tillet and Francis 1930). CRP molecules from all species display a property of Ca^{2+} -dependent binding to PC. A rCRP molecule is composed of five identical subunits arranged as a cyclic pentamer with PC binding sites on one side. Although a PC group is a polar head of a major lipid in cell membranes, CRP molecules only bind to necrotic cells and invading microbes (Volanakis and Wirtz 1979). The binding complexes initiate a classic C pathway, influencing the activities of

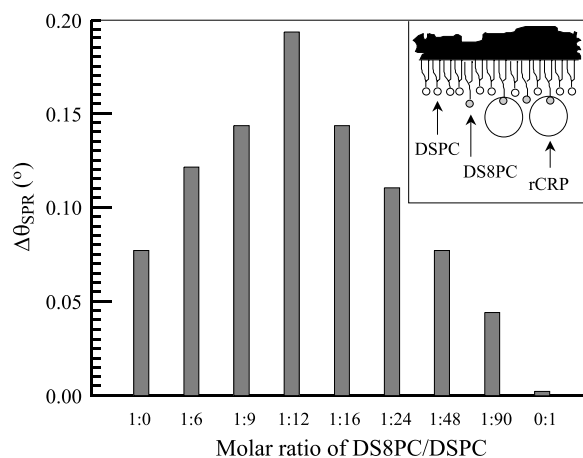


Fig. 6 Specific interactions of rabbit C-reactive protein (rCRP) with different molar ratios for the DS8PC/DSPC monolayer. On the monolayer of molar ratio 1:12 there was a maximum adsorption, $\Delta\theta_{\text{SPR}} = 0.193^\circ$. The inset is a drawing of two rCRP molecules specifically binding to a DS8PC/DSPC monolayer transferred onto a gold film

platelets and lymphocytes. The recognition and binding mechanism of CRP with its substrates is not clear. Using three synthesized lipids with longer polar heads and the SPR technique, information about steric hindrance between rCRP and phospholipid monolayers was obtained.

Natural lipid DSPC and a synthesized lipid were mixed in a given molar ratio. After the mixed monolayer was transferred to a gold film, the sensitive chip was installed in the SPR system. The sample chamber was then installed and filled with 150 μl buffer containing 2 mM EDTA. After rCRP (2 μl , 0.7 mg/ml) was injected into the chamber, no change of θ_{SPR} was observed. Because one EDTA molecule binds with one calcium ion, 50 μl buffer containing 10 mM CaCl_2 was added to the chamber. θ_{SPR} increased only when DS8PC molecules were present inside the sensitive chips. The change of θ_{SPR} was dependent on the molar ratios of DS8PC and DSPC in the supported monolayers (Fig. 6). After 60 min the adsorption of rCRP on a DS8PC/DSPC monolayer became saturated. After 10 μl buffer containing 20 mM PC was added to the chamber, θ_{SPR} quickly decreased almost to the position before the CaCl_2 was added. If the rCRP liquid was first incubated with PC, then the rCRP could not react with monolayers containing DS8PC. As the reaction of rCRP with DS8PC/DSPC monolayers was dependent on Ca^{2+} , and the reaction could be inhibited by PC, the interactions in the above experiments were specific.

A molecule of DS8PC in the monolayer acts as a receptor for rCRP molecule. The more DSPC molecules were mixed with DS8PC in a monolayer, the more lateral space was occupied by a polar head of a DS8PC, and more rCRP molecules could bind to the monolayer. At the molar ratio 1:12, the DS8PC/DSPC monolayer had maximum adsorp-

tion to rCRP ($\Delta\theta_{\text{SPR}}=0.193^\circ$). A rCRP molar mass is 1.2×10^5 g/mol. From Eq. (5) it was obtained that the average transverse area of one rCRP molecule on the monolayer surface was $10\,400 \text{ \AA}^2$. From electron microscope observations the diameter of one rCRP molecule was found to be about 100 \AA . Therefore a square area of one observed rCRP molecule agreed with the above SPR experimental result. This meant that the DS8PC/DSPC monolayer with a molar ratio of 1:12 could be covered by rCRP molecules almost completely. If the ratio of DS8PC/DSPC was smaller than 1:12, receptors in the monolayer become relatively fewer, so that the amount of rCRP binding to the monolayer decreased.

The recent publication of a human CRP X-ray structure (Shrive et al. 1996) indicated that a PC binding site in a CRP subunit was in a pocket. In the above experiments, DP3PC/DSPC and DS6PC/DSPC monolayers could not react with rCRP. Flexible polar heads of DS8PC molecules in a DS8PC/DSPC monolayer might protrude far enough to reach PC binding sites of rCRP molecules. From the chemical formulae of DS8PC and DSPC, the depth of a PC binding pocket in a rCRP molecule was presumed to be about 10 \AA .

Conclusions

A SPR system is just like an optical amplifier. While an organic film was assembling on a gold film, a shift of a SPR spectrum resonance angle was directly proportional to the product of the thin organic film thickness and the refractive index difference between the thin organic film and the buffer containing the sample. It was also found that $\Delta\theta_{\text{SPR}}$ was not sensitive to the sample support of a gold film and a glass cover slip. From $\Delta\theta_{\text{SPR}}$ and the derived formulae, a sample molecule length, transverse area, surface concentration and surface density could be quantitatively evaluated. From these data, the interactions of protein and phospholipid and the hybridization of oligonucleotides could be quantitatively monitored in real time.

In order to obtain the sample layer thickness from Eq. (1), the index difference between a sample and a buffer containing the sample must be known. The formula was only suitable for layers in which sample molecules compacted tightly, because the refractive indexes of this kind of biological layer can be obtained from other sources. In order to obtain a sample surface concentration from Eq. (2),

the ratio of the sample volume concentration to the refractive index difference between the sample and the buffer soaking the sample should also be known. Because the ratio for protein samples is almost constant, Eqs. (3)–(5) for σ , N and S could be widely used for protein samples in the homemade SPR system. They might also be suitable for phospholipid monolayer and oligonucleotides strands. From the program used, the same kind of formulae for σ , N and S could also be obtained for any SPR system with a different optical layout.

Acknowledgements It is pleasure to acknowledge valuable experimental supports and suggestions by Dr. Han Xuehai and Mrs. Ma Hong. Some of the SPR numerical simulations were finished in the Department of Physical and Astronomical Sciences of the University of Palermo, Italy. I am grateful Prof. M. U. Palma for his critical reading and his useful suggestions for the manuscript. I am equally grateful to Dr. P. L. San Biagio for his support.

References

- Chapman D (1968) Biological membranes, physical fact and function. Academic Press, London, p 99
- Chapman D, Wallach DFH (1973) Biological membranes, vol 2. Academic Press, London, pp 8–9
- Liedberg B, Nylander C, Lundström I (1995) Biosensing with surface plasmon resonance – how it all started. *Biosens Bioelectron* 10:i–ix
- Liu Z, Xiao C, Sui SF, et al. (1995) Specific binding of avidin to biotin containing lipid lamella surfaces studied with monolayers and liposomes. *Eur Biophys J* 24:31–38
- Qin H, Liu Z, Sui S-F (1995) Two-dimensional crystallization of avidin on biotinylated lipid monolayers. *Biophys* 68:2493–2496
- Raether H (1989) Surface plasmons on smooth and rough surfaces and gratings. (Springer tracts in modern physics, vol 111) Springer, Berlin Heidelberg New York, pp 1–30
- Salamon Z, Wang Y, Soulages JL, Brown MF, Tollin G (1996) Surface plasmon resonance spectroscopy studies of membrane proteins: transducin binding and activation by rhodopsin monitored in thin membrane films. *Biophys J* 71:283–294
- Sheila JW (1993) DNA-DNA hybridization in real time using BIAcore. *Microchem* 47:330–337
- Shrive AK, et al. (1996) Three dimensional structure of human C-reactive protein. *Nat Struct Biol* 4:346–354
- Stenberg E, Persson B, Roos H, Urbaniczky C (1991) Quantitative determination of surface concentration of protein with surface plasmon resonance using radiolabeled protein. *J Colloid Interface Sci* 143:513–526
- Swanson SJ, Mortensen RF (1990) *Mol Immunol* 27:679–687
- Tillett WS, Francis T (1930) Serological reaction reactions in pneumonia with a non-protein somatic fraction of pneumococcus. *J Exp Med* 52:561–571
- Volanakis JE, Wirtz KWA (1979) Interaction of C-reactive protein with artificial phosphatidylcholine bilayers. *Nature* 218: 155–157